

Experimental Analysis of Out-of-plane Behavior of Masonry Infill Walls Strengthened with Textile Reinforced Mortar and Wall Post in Autoclaved Aerated Concrete Frames

Rezgar Boukani¹, Masood Farzam², Kaveh Nezamisavojbolaghi^{1*}, Aladdin Behraves²

¹ Faculty of Civil Engineering, Islamic Azad University, Mahabad 5913933137, Iran

² Faculty of Civil Engineering, University of Tabriz, Tabriz 5166616471, Iran

* Corresponding author, e-mail: k.nezami@iau-mahabad.ac.ir

Received: 26 February 2023, Accepted: 18 January 2024, Published online: 18 March 2024

Abstract

An experimental study was carried out to contribute to the rather limited data on the out-of-plane (OOP) behavior of masonry infills in reinforced concrete (RC) frames strengthened with the wall post and the textile-reinforced mortar (TRM). For this purpose, one unreinforced specimen served as the control, one specimen was reinforced with the wall post, and two specimens were reinforced with the TRM. They were fabricated and subjected to cyclic OOP loading until a drift ratio of 6%. Load and displacement values were recorded, and the research team discussed the failure mechanisms of the specimens. Results showed that the application of the wall post had the highest efficiency as it increased the load by about 3 times, while this value for TRM-strengthened walls was only 1.5. Strengthening modified the cracking, shifting it towards the middle parts of the wall, changing it from a brittle to a failure mode. Comparison of the envelope curves of specimens revealed significant improvements. The ultimate displacement and energy absorption capacity for the specimen reinforced with the post wall increased by 30% and 300% respectively. Similarly, for TRM-strengthened specimens, these values were 48% and 100%.

Keywords

out-of-plane (OOP) behavior, masonry infill walls, RC frames, textile reinforced-mortar (TRM), post wall, strengthening, autoclaved aerated, concrete (AAC)

1 Introduction

In many regions of the world, there are buildings that have not been designed according to the seismic requirements of design codes. A group of such structures which perform poorly under seismic loadings relate to reinforced concrete frames with masonry infills. Despite the fact that masonry infills increase the lateral capacity of such frames, it has been proven that they are more susceptible to failure against loads perpendicular to their plane [1–3]. The out-of-plane (OOP) failure of a wall has been studied in the past years, all concluding that this type of failure is more disastrous than the in-plane (IP) failure [4, 5]. IP failure is mainly characterized by the combination of several local failures, namely, corner crushing, diagonal compression, frame failure, bed-joint sliding, and diagonal cracking [6–8]. Many factors play a role in the mechanical performance of masonry-infilled reinforced concrete (RC) structures. Some of these factors include but are not limited to modulus of elasticity, tensile strength, and compressive strength of the infill,

the inter-layer strength between masonry blocks (i.e., brick-mortar interface), as well as the mechanical properties of the surrounding RC frame [6, 9]. Friction and stiffness between the infill and the interface, their connection and their stiffness relative to one another also play an undeniable role in the IP failure of infilled frames [10]. Furthermore, the location and geometry of other parameters, such as openings in the infill wall, affect the IP strength of the wall and modify the failure pattern [11]. Needless to say, the OOP strength of the wall decreases if it sustains IP lateral loading. What's more, the vulnerability of the wall to the imposed loads increases if there is no connection between the RC frame and the infill wall and/or the support width of the panel is inadequate. The outcome of these phenomena indicates that the OOP strength of the infilled frames reduces with the increasing slenderness of the wall [12]. Moreover, the IP-OOP interaction behavior is also a governing factor as it negatively affects the OOP strength capacity [1, 3].

Boundary conditions of the wall which directly play a role in its failure mechanism and OOP strength is another factor that should be accounted for [13, 14]. In addition, workmanship could affect the IP and OOP response factors by 30% [15]. It is noteworthy that existing regulations have not demanded specific detailing for the strengthening of infill walls. Textile-reinforced mortar (TRM) is a matrix consisting of concrete or lime, which in combination with the textile mesh made of various reinforcing fibers, is a popular solution for its low cost, ease of applicability, and adaptability with RC or masonry structures given. Their durability features and minimal thickness in comparison with other methods of strengthening such as jacketing [16]. Meanwhile, the use of an inorganic matrix such as TRM in lieu of epoxy resins such as FRPs relieves the user of the FRP drawbacks (inconsistency with the substrate material, infeasibility to apply to wet surfaces, high cost, etc.).

1.1 Background on masonry-infilled RC frame retrofitted with TRM

Out of many objectives, the two primary objectives for using TRMs are (I) minimizing the vulnerability of wall against OOP loading and (II) contributing to the IP lateral capacity. In the following, some of the studies that have attempted to characterize the behavior of masonry-infilled RC frames strengthened with TRM will be discussed in brief. A comprehensive study was carried out by da Porto et al. [17] to investigate the IP-OOP interaction behavior of eight full-scale, one-story, one-bay RC frames with non-structural infills strengthened with different TRMs consisting of basalt, glass, and steel fibers under monotonic loading. The walls were 4150 mm in height, 2650 mm in length, and a slenderness ratio of 22.08 made of clay bricks with a thickness of 120 mm. TRMs contributed to energy absorption (20%), less damage, and ductile behavior. Using TRMs improved the OOP capacity by 3.5 times. In a similar study by Minotto et al. [18] highlighted the significance of using TRM as using it changes the failure mode from brittle to ductile. It was also highlighted that studies on the IP-OOP interaction behavior of masonry infilled RC frames are scarce. De Risi et al. [19] conducted experimental studies on one-bay one-story full-scale models where a wall of 4200 mm in length, 2300 mm in width, and slenderness of 20.91 was subjected to pure OOP loading. Applying TRMs contributed to strain gain by 1.77–2.22 times and the dissipated energy increased by 1.93 times. Furtado et al. [20] tested walls similar to that of De Risi et al. [19] with the exception that the slenderness of the wall was 15.33 in this case. High-strength and medium-strength TRMs

combined with steel and plastic connectors were used. The novelty of the work was that authors had used steel plates to distribute the connection area of textile mesh to the frame and steel connectors which prevented debonding and separation of the textile mesh. High-strength textile meshes didn't improve the OOP strength notably. Overall, utilization of TRMs improved the ultimate strength by 1.75–2.44 times, initial stiffness by 4 times, deformation capacity by 2.72 times and energy absorption by a minimum of 2 times compared with control specimens. De Risi et al. [21] tested four full-scale masonry-infilled (hollow clay bricks and common mortars for bed joint) RC frames in two conditions (1) pure OOP loading, and (2) IP- OOP loading. Masonry bricks with a thickness of 110 mm, width of 300 mm, height of 200 mm and slenderness ratio of 20.91 were enclosed in a 4800 mm long, and 3300 mm high RC frame for beams tested under pure OOP loading, utilization of glass fiber-reinforced TRMs improved the initial stiffness by 5.33 times and the strength by 44%, and 78% for specimens with/without previous IP damage, respectively. Improvements in the energy absorption capacity of the wall were 50–100%. Last but not least, the authors highlighted the need for further research to investigate the OOP behavior of masonry infilled RC frames. A holistic review of the existing literature as well as a comprehensive review by Filippou et al. [22] reveal that studies regarding the OOP behavior of masonry walls strengthened with TRMs are few and more studies are required in this regard. To contribute to enriching the existing literature in this regard the authors have carried out experimental studies on autoclaved aerated concrete (AAC) concrete frames with masonry infills strengthened with TRM, and post wall and have compared the results with the control specimen.

2 Experimental program

2.1 ACC blocks

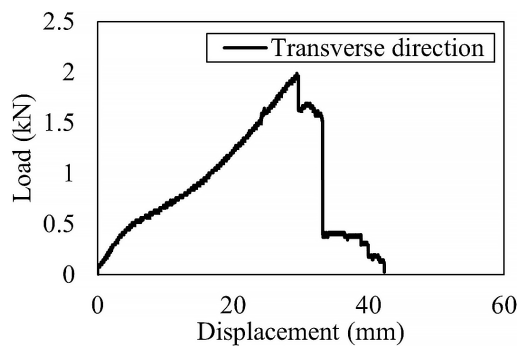
AAC blocks used in this study were 600 mm in length, 200 mm in height, and 240 mm in width. They had a compressive strength of 3.1 MPa, modulus of elasticity equal to 2.25 GPa, and a density of 0.55 g/cm³.

2.2 Geogrid

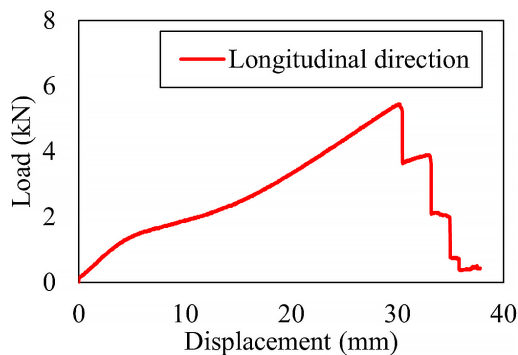
The geogrid utilized in the present investigation is presented in Fig. 1. It had a width of 550 mm, while its longitudinal and transverse ribs had lengths of 25 mm and 35 mm, respectively. The maximum strain was determined to be 0.12. The tensile test results shown in Fig. 2 indicate that the geogrid could withstand loads of 5.5 kN and 2 kN in the transverse and longitudinal directions, respectively.



Fig. 1 The geogrid used in the current study



(a)



(b)

Fig. 2 Load-displacement response of geogrid (a) transverse direction, and (b) longitudinal direction

2.3 Masonry walls

Masonry walls had dimensions of 3000×2250×200 mm and 25 AAC blocks were used to build the wall. Relevant information for each wall is given in Table 1.

2.4 AACW specimen

In the AACW wall, bonding between the blocks of this wall was provided with a mortar composition having a thickness of 2 mm, and interface strength (i.e., cohesion) of 0.3 MPa. To provide a rigid connection between the ground floor and the specimen, two No. 10 angles were used and to create a uniform load distribution, two

Table 1 Specifications of test specimens

| Specimen ID | Comments |
|-------------|---|
| AACW | Reference specimen |
| AACWRS | Strengthened with wall post |
| AACWRT-II-1 | Strengthened with TRM in two vertical rows at both ends of the wall |
| AACWRT-II-2 | AACWRT-II-1 repeated |

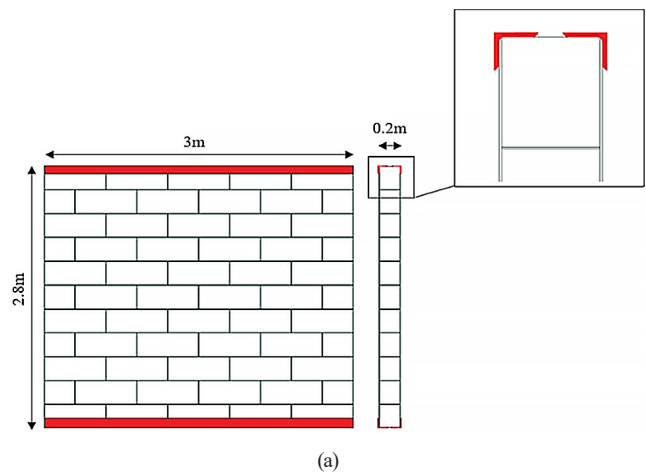
No. 8 angles were used at top of the wall where the OOP load was applied according to Fig. 3.

2.5 AACWRS specimen

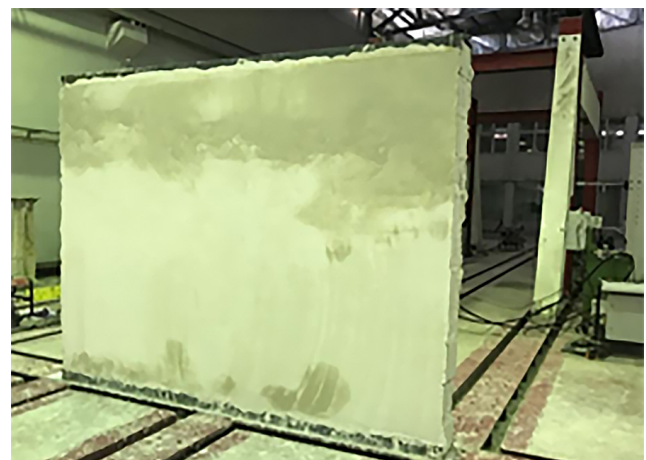
Two No. 8 angles were used with steel belts of 3 mm in thickness on both ends of the wall. Detailing of angles positioning as well as the test specimen are given in Fig. 4.

2.6 AACWRT specimens

Two rows of geogrid were wrapped around the wall at its both ends and were fixed in place with a common gypsum.



(a)



(b)

Fig. 3 AACW specimen (a) schematic view (unit: meter), and (b) real test specimen

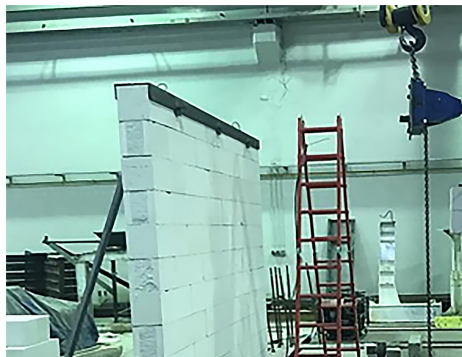
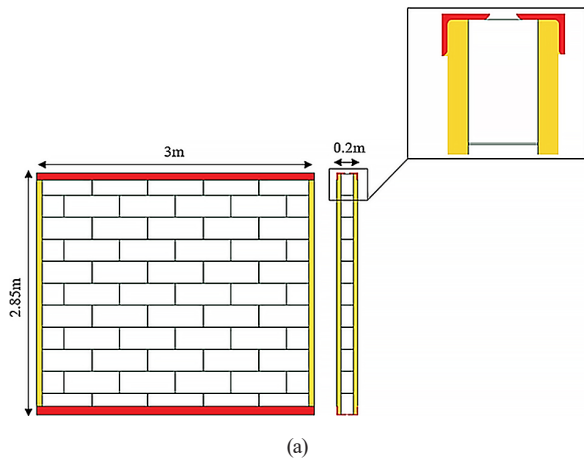


Fig. 4 AACWRS specimen (a) schematic view (unit: m), (b) real test specimen, (c) perimeter connection of wall with angles

It is noteworthy that, two No. 8 angles were used to apply a distributed load subsequent to application of geogrid on AAC blocks. Fig. 5 shows the details of the work.

3 Loading protocol

Cyclic loading was applied at the highest elevation of the to reach the drift ratio of 6% using a 1000 kN hydraulic jack according to the loading protocol of Fig. 6. Each complete cycle step consisted of two cyclic loadings (amounting to 262 steps in total), with an increment of 6 mm in each sub-step. Load values and its corresponding displacements were recorded in each step of loading. Fig. 7 shows the test setup and loading of specimen AACW. Displacement was measured by the internal linear variable displacement transducer (LVDT) of the loading jack which was used to apply loading to top of the wall.

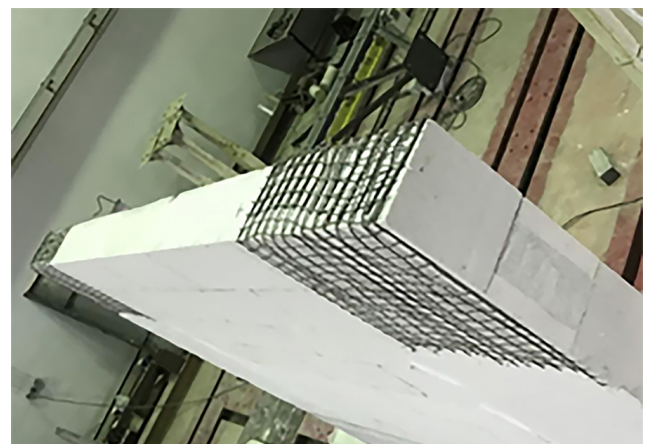


Fig. 5 AACWRT specimen (a) schematic view (unit: meter), (b) real test specimen, and (c) detailing on top of the wall

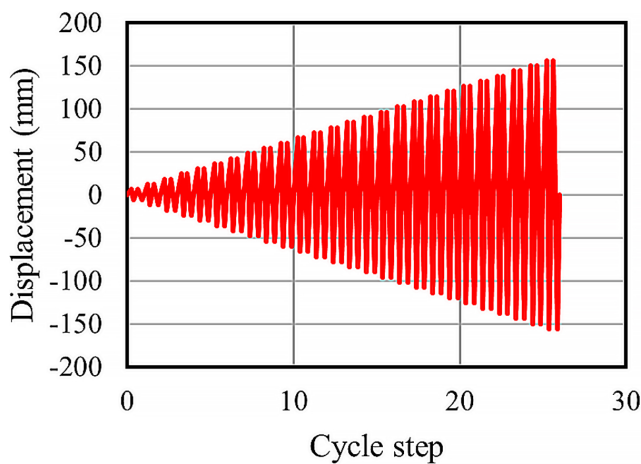


Fig. 6 Displacement-controlled loading protocol

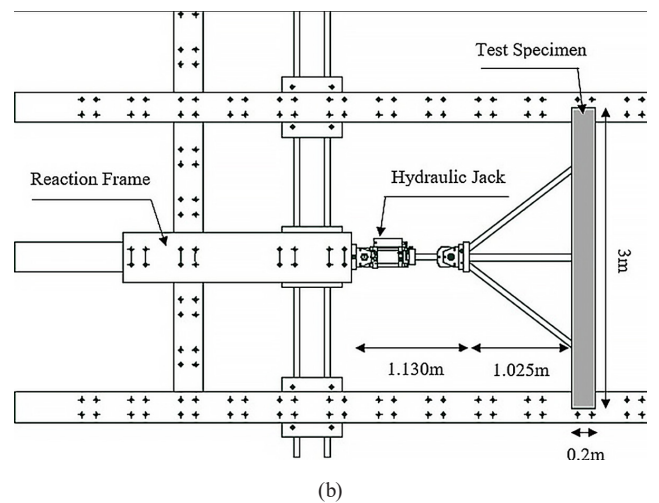
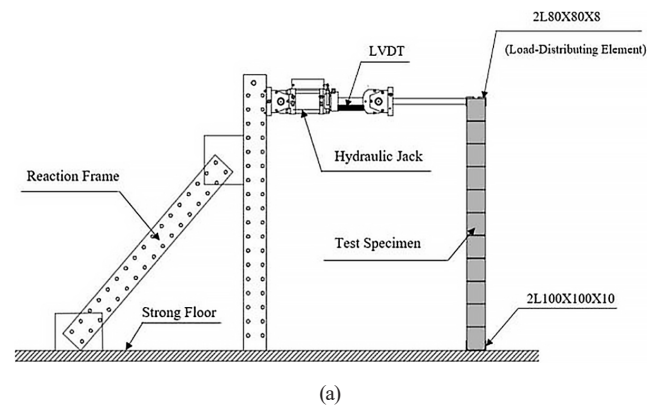
4 Results and discussions

4.1 Specimen AACW

Fig. 8 shows the deformed shape and failure pattern of AACW specimen. Upon increase of deformation of the wall, cracks initiated from the external corners of the first row of bricks at the bottom of the wall and propagated to the middle of the wall according to Fig. 8 (b) and (c). Further loading was characterized by the appearance of longitudinal crack at top of the wall, beneath the angle to which the load was applied Fig. 8 (d). Thereafter, initial cracks at the bottom of the wall widened and propagated until the wall failed Fig. 8 (e). Based on the force-displacement curve of specimen AACW given in Fig. 9, the initial part of the curve is linear until it reaches a peak load of 1.85 kN before dropping notably, undergoing a load plateau while displacements increase. Thereafter, the load drops suddenly to a value of 0.2 kN and fluctuates as the displacement values reach 110 mm. Given the overall trend, it is clear that the failure of the AACW specimen is brittle and the peak load value is its ultimate load capacity.

4.2 Specimen AACWRS

Fig. 10 (a) shows cracking of specimen AACWRS at various stages of loading. Unlike specimen AACW, initial cracks started at the outer corner of the second row of blocks and propagated towards the inner parts of the wall. Next, first row cracked as well followed by the formation of cracks at top of the wall beneath the angles to which the load was applied and thereafter, emergence of vertical cracks at the masonry blocks of the first row at the bottom of the wall. Unlike the force-displacement trend of specimen AACW, in specimen AACWRS (Fig. 11), initial linear reversed cyclic loading was not followed by a



(c)

Fig. 7 (a) side view sketch of test setup, (b) top view sketch of test setup, and (c) loading of specimen AACW

sudden drop of the load capacity but in contrast, displacement-hardening was observed given the presence of post-wall strengthening until the specimen reached a rough load capacity of 6 kN, sustained this load value for almost

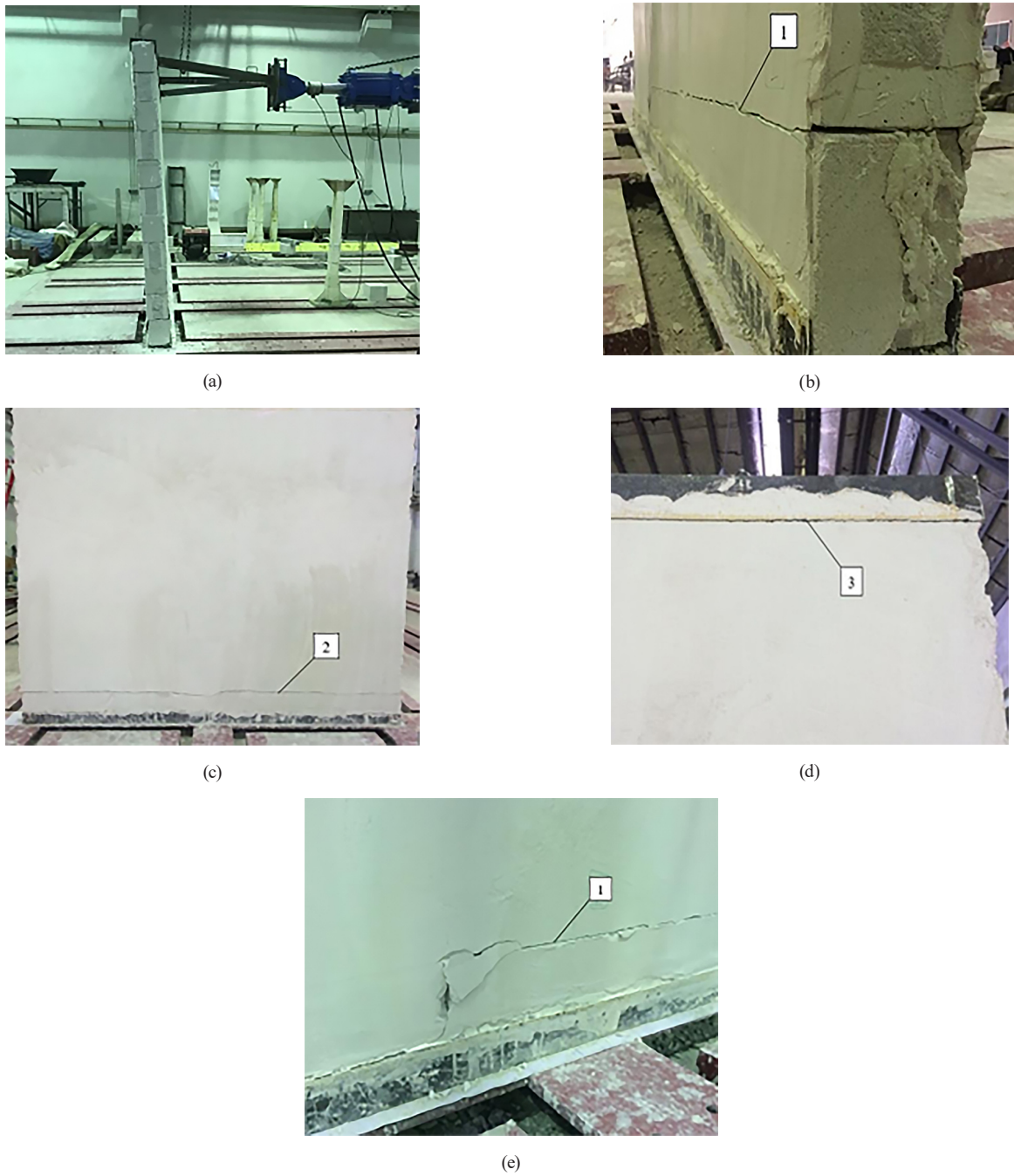


Fig. 8 Specimen AACW (a) deformed shape of the wall, (b) crack propagation along thickness, (c) propagation of cracks along the length of the wall, (d) appearance of cracks at the top of the wall beneath the angle to which load was applied, and (e) widening of cracks at the bottom of the wall

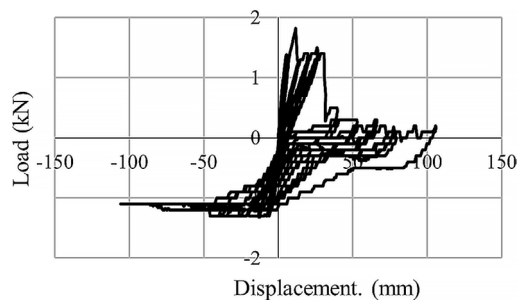


Fig. 9 Force-displacement curve of specimen AACW

30 mm, before failing at 150 mm. Failure mode of the specimen was not brittle and the failure occurred gradually by the distribution of cracks.

4.3 Specimen AACWRT-II-1 & 2

Fig. 12 shows the loading as well as the evolution of crack at various stages of loading. Primary cracks initiated at the first and second rows of blocks, followed by the emergence of the cracks at top of the wall and finally exposure

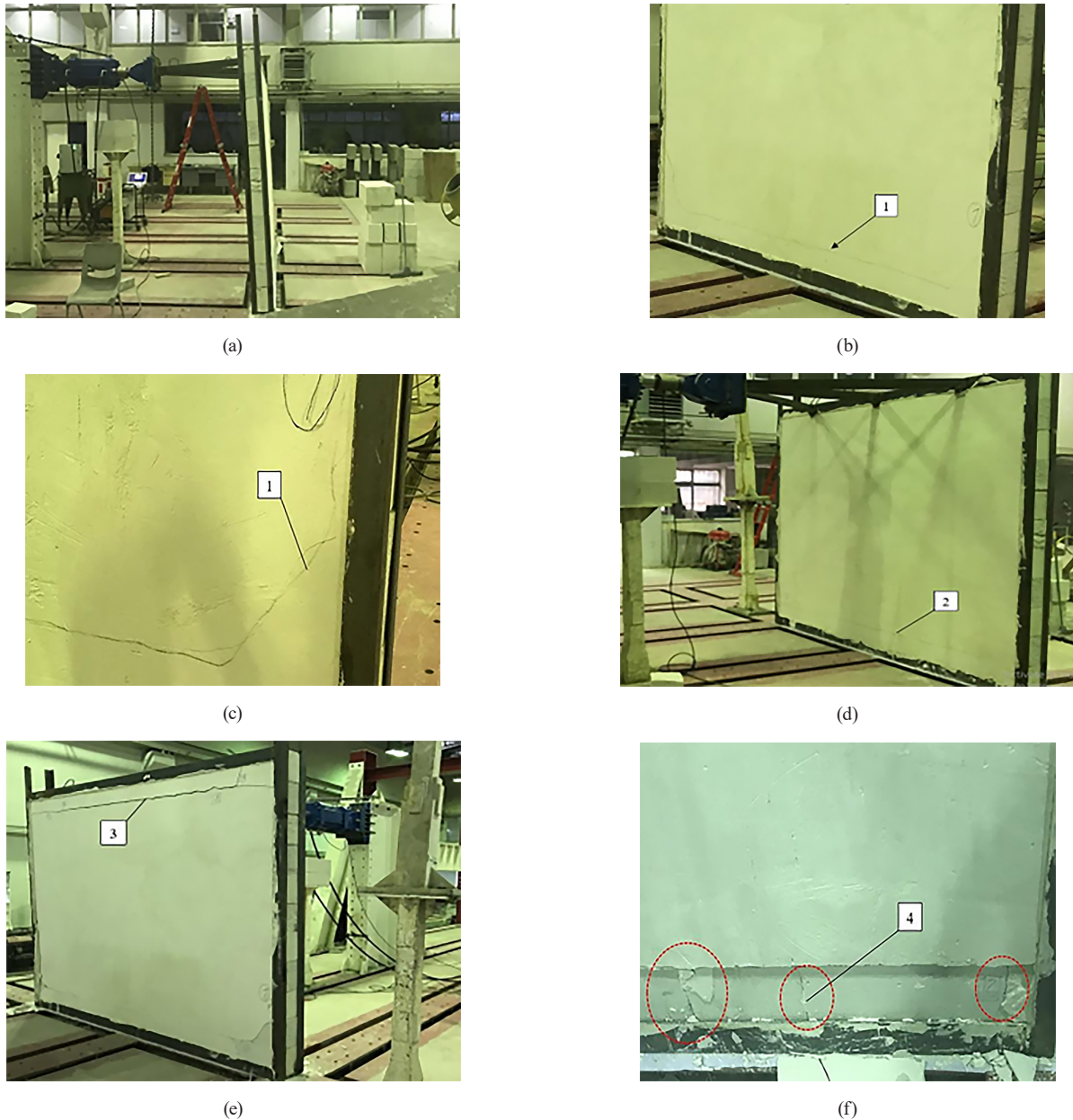


Fig. 10 Specimen AACWRS (a) deformed shape of the wall, (b) formation of initial cracks at the second row of the wall, (c) propagation of cracks to the middle parts of the wall, (d) appearance of cracks at the first row of masonry blocks, (e) cracking of the wall at the top beneath the angles to which the load was applied (f) vertical cracks along the masonry blocks at the first row

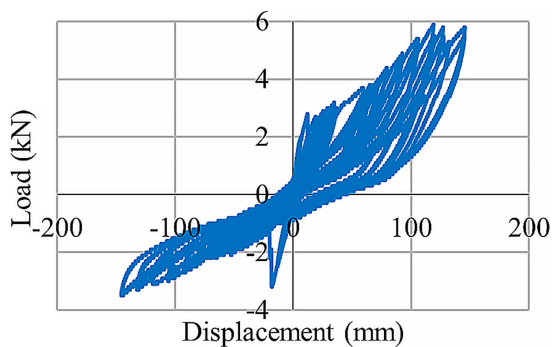


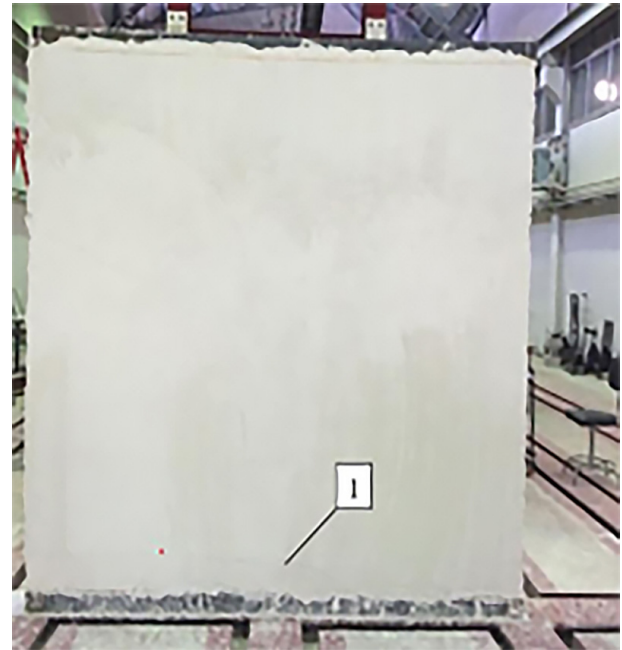
Fig. 11 Force-displacement curve of specimen AACWRS

of TRM by the spalling that occurred at the bottom of the wall.

Fig. 13 shows the force-displacement curve of specimens reinforced with TRM. In these specimens similar to specimen AACWRS, failure of the wall was ductile characterized by displacement-hardening behavior of the wall after the first cycle followed by a stable and/or slight decreasing trend of the specimen to reach displacement values of 150 mm. This gradual evolution of cycles at relatively large load values indicates the energy absorption capacity of the walls



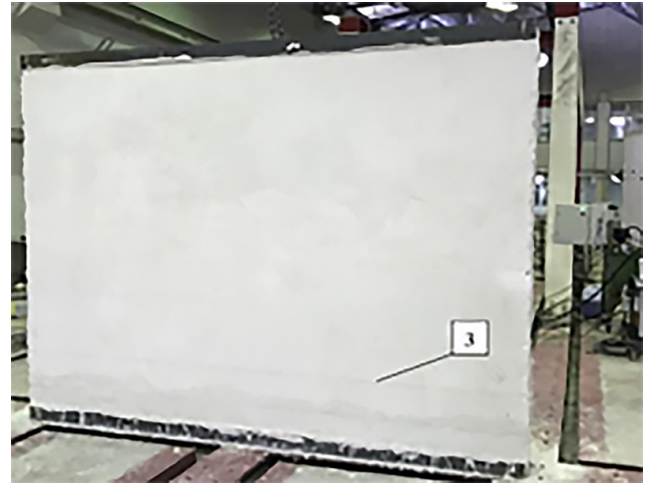
(a)



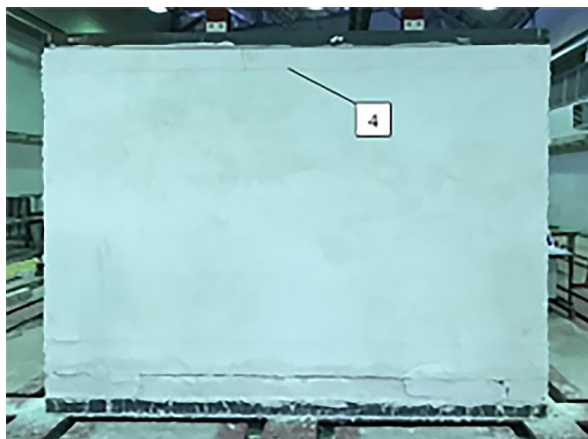
(b)



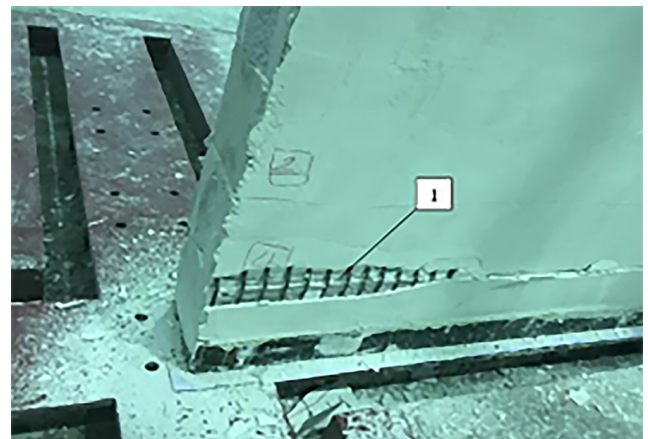
(c)



(d)



(e)



(f)

Fig. 12 Specimens AACWRT (a) deformed shape of the wall, (b) emergence of cracks at the first row of masonry blocks, (c) cracks on the front face (loading face), (d) cracks on the back face, (e) presence of cracks at top of the wall beneath the angle to which the load was applied, (f) exposure of TRM due to spalling of gypsum

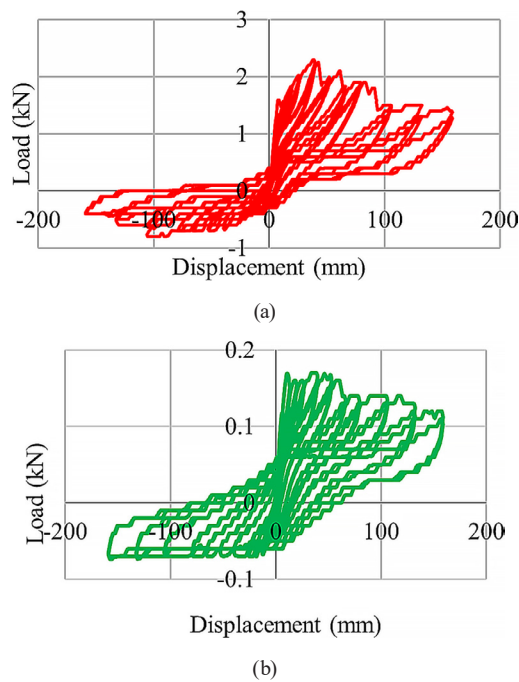


Fig. 13 Force-displacement curves of specimen AACWRT
(a) AACWRT-1, and (b) AACWRT-2

and their ability to deform adequately, giving signals to its failure rather than a sudden brittle failure.

Fig. 14 shows the envelope curves of all the test specimen. It is observed that the AACWRS specimen has shown both the highest load value and energy absorption followed by TRM-reinforced specimens. It is clear from Table 2 (based on envelope curves) that application of TRM didn't contribute to the initial stiffness of the curves while the converse was true for the specimen strengthened with post walls; an increase of 27% in initial stiffness of the curve relative to the control specimen was witnessed. AACWRS specimen sustained load values as high as 3 times relative to the control specimen; this value for TRM-strengthened specimens was 1.5. Displacement-hardening behavior was also observed in all the specimens except for the control specimen which was mainly due to the presence of steel angles at the perimeter of the wall. The ultimate displacement ($\Delta_{Ultimate}$) improved by 30%, and 48% for specimens AACWRS and AACWRT, respectively. Similarly, energy absorption (E) values increased by 4 and almost 2 times for specimens AACWRS, and AACWRT, respectively.

5 Conclusions

An experimental study was carried out to investigate the out-of-plane (OOP) behavior of masonry infills in RC frames. To this end, one unreinforced masonry specimen,

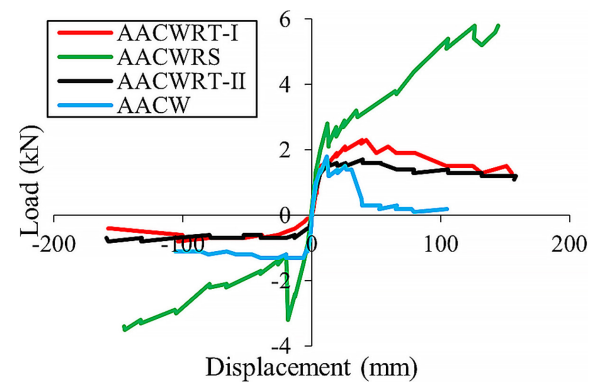


Fig. 14 Envelope curves of all test specimens

Table 2 Summary of test results

| Specimen ID | Stiffness (N/m) $\times 10^5$ | Peak (kN) | $\Delta_{Ultimate}$ | Ductility ($\times 10^{10}$) | E (N.m) $\times 10^2$ |
|-------------|----------------------------------|--------------|---------------------|-----------------------------------|--------------------------|
| AACW | 3.205 | 1.50 | 104.670 | --- | 1.881 |
| AACWRS | 4.088 | 5.80 | 144.840 | 5.510 | 9.144 |
| AACWRT-II-1 | 2.177 | 2.30 | 155.230 | 2.340 | 3.492 |
| AACWRT-II-2 | 1.960 | 1.70 | 156.840 | 2.370 | 3.280 |

one specimen reinforced with the wall post, and two specimens reinforced with the TRM were tested under cyclic loading until a drift ratio of 6%. Based on the results, the salient findings of the current study are as follows:

1. Strengthening of the wall modified the cracking and failure pattern of the wall from a brittle to ductile.
2. The wall-post strengthening method proved to be the most efficient by improving the load capacity to 3 times higher, while for the TRM, this improvement was only 50%.
3. Displacement-hardening behavior was observed in strengthened specimens given the presence of steel angles at the perimeter of the wall.
4. The ultimate displacement ($\Delta_{Ultimate}$) was enhanced by 30% and 48% for specimens AACWRS and AACWRT, respectively. Similarly, energy absorption (E) values increased by 4 and almost 2 times for specimens AACWRS and AACWRT, respectively.
5. Envelope curves of the specimens upon reverse cyclic loading are asymmetric, i.e., different behavior is observed in the 1st and 3rd quadrants after the linear branch in initial cycles.

6 Recommendations for future work

It is recommended that different configurations of TRM, for example, continuous utilization of TRMs over the surface but with larger apertures, be used. Another parameter

worth investigating is the use of different types of textiles for strengthening. The third development in the work could involve investigating different types of blocks or mortar.

References

- [1] Furtado, A., Rodrigues, H., Arêde, A., Varum, H. "Experimental evaluation of out-of-plane capacity of masonry infill walls", *Engineering Structures*, 111, pp. 48–63, 2016.
<https://doi.org/10.1016/j.engstruct.2015.12.013>
- [2] Palieraki, V., Zeris, C., Vintzileou, E. Adami, C. "In-plane and out-of plane response of currently constructed masonry infills", *Engineering Structures*, 177, pp. 103–116, 2018.
<https://doi.org/10.1016/j.engstruct.2018.09.047>
- [3] Ricci, P., Di Domenico, M., Verderame G. M. "Experimental assessment of the in-plane/out-of-plane interaction in unreinforced masonry infill walls", *Engineering Structures*, 173, pp. 960–978, 2018.
<https://doi.org/10.1016/j.engstruct.2018.07.033>
- [4] Hermanns, L., Fraile, A., Alarcón, E., Álvarez, R. "Performance of buildings with masonry infill walls during the 2011 Lorca earthquake", *Bulletin of Earthquake Engineering*, 12(5), pp. 1977–1997, 2014.
<https://doi.org/10.1007/s10518-013-9499-3>
- [5] De Luca, F., Verderame, G. M., Gómez-Martínez, F., Pérez-García, A. "The structural role played by masonry infills on RC building performances after the 2011 Lorca, Spain, earthquake", *Bulletin of Earthquake Engineering*, 12(5), pp. 1999–2026, 2014.
<https://doi.org/10.1007/s10518-013-9500-1>
- [6] Chrysostomou, C. Z., Asteris, P. G. "On the in-plane properties and capacities of infilled frames", *Engineering Structures*, 41(02), pp. 385–402, 2012.
<https://doi.org/10.1016/j.engstruct.2012.03.057>
- [7] Shing, P. B., Koutromanos, I., Stavridis, A. "Seismic performance of masonry-infilled RC frames with and without retrofit", *Journal of Earthquake and Tsunami*, 7(03), 1350023, 2013.
<https://doi.org/10.1142/S1793431113500231>
- [8] Jin, H., Jin, X., Dai, J. "Analysis on failure modes and numerical simulations of masonry-infilled reinforced concrete frame structures", *China Civil Engineering Journal*, 47(S2), pp. 175–180, 2014.
- [9] Calvi, G. M., Bolognini, D. "Seismic response of reinforced concrete frames infilled with weakly reinforced masonry panels", *Journal of Earthquake Engineering*, 5(02), pp. 153–185, 2001.
<https://doi.org/10.1080/13632460109350390>
- [10] Shing, P. B., Mehrabi, A. B. "Behaviour and analysis of masonry-infilled frames", *Progress in Structural Engineering and Materials*, 4(3), pp. 320–331, 2002.
<https://doi.org/10.1002/pse.122>
- [11] Kakaletsis, D. J., Karayannis C. G. "Influence of masonry strength and openings on infilled R/C frames under cycling loading", *Journal of Earthquake Engineering*, 12(2), pp. 197–221, 2008.
<https://doi.org/10.1080/13632460701299138>
- [12] De Risi, M. T., Di Domenico, M., Ricci, P., Verderame, G. M., Manfredi, G. "Experimental investigation on the influence of the aspect ratio on the in-plane/out-of-plane interaction for masonry infills in RC frames", *Engineering Structures*, 189, pp. 523–540, 2019.
<https://doi.org/10.1016/j.engstruct.2019.03.111>
- [13] Tondelli, M., Beyer, K., DeJong, M. "Influence of boundary conditions on the out-of-plane response of brick masonry walls in buildings with RC slabs", *Earthquake Engineering & Structural Dynamics*, 45(8), pp. 1337–1356, 2016.
<https://doi.org/10.1002/eqe.2710>
- [14] Di Domenico, M., Ricci, P., Verderame, G. M. "Experimental assessment of the influence of boundary conditions on the out-of-plane response of unreinforced masonry infill walls", *Journal of Earthquake Engineering*, 24(6), pp. 881–919, 2020.
<https://doi.org/10.1080/13632469.2018.1453411>
- [15] Akhoundi, F., Vasconcelos, G., Lourenço, P. "Experimental out-of-plane behavior of brick masonry infilled frames", *International Journal of Architectural Heritage*, 14(2), pp. 221–237, 2018.
<https://doi.org/10.1080/15583058.2018.1529207>
- [16] Verderame, G. M., Balsamo, A., Ricci, P., Di Domenico, M., Maddaloni, G. "Experimental assessment of the out-of-plane response of strengthened one-way spanning masonry infill walls", *Composite Structures*, 230, 111503, 2019.
<https://doi.org/10.1016/j.compstruct.2019.111503>
- [17] da Porto, F., Guidi, G., Verlato, N., Modena, C. "Wirksamkeit von putz und textilbewehrtem mörtel bei der verstärkung von ausfachungswänden aus ziegelmauerwerk, die kombinierter schein-und plattenbeanspruchung ausgesetzt sind", (Effectiveness of plasters and textile reinforced mortars for strengthening clay masonry infill walls subjected to combined in-plane/out-of-plane actions), *Mauerwerk*, 19(5), pp. 334–354, 2015. (in German)
<https://doi.org/10.1002/dama.201500673>
- [18] Minotto, M., Verlato, N., Donà, M., da Porto, F. "Strengthening of in-plane and out-of-plane capacity of thin clay masonry infills using textile- and fiber-reinforced mortar", *Journal of Composites for Construction*, 24(6), 04020059 2020.
[https://doi.org/10.1061/\(ASCE\)CC.1943-5614.0001067](https://doi.org/10.1061/(ASCE)CC.1943-5614.0001067)
- [19] De Risi, M. T., Furtado, A., Rodrigues, H., Melo, J., Verderame, G. M., António, A., Varum, H., Manfredi, G. "Experimental analysis of strengthening solutions for the out-of-plane collapse of masonry infills in RC structures through textile reinforced mortars", *Engineering Structures*, 207, 110203, 2020.
<https://doi.org/10.1016/j.engstruct.2020.110203>
- [20] Furtado, A., Rodrigues, A., Arede, A., Melo, J., Varum, H. "Composite structures", 255, 113029, 2021.
<https://doi.org/10.1016/j.compstruct.2020.113029>
- [21] De Risi, M. T., Furtado, A., Rodrigues, H., Melo, J., Verderame, G. M., Arêde, A., Varum, H., Manfredi, G. "Influence of textile reinforced mortars strengthening on the in-plane/out-of-plane response of masonry infill walls in RC frames", *Engineering Structures*, 254, 113887, 2022.
<https://doi.org/10.1016/j.engstruct.2022.113887>
- [22] Filippou, C., Furtado, A., Risi, M. T., Kyriakides, N., Chrysostomou, C. Z. "Behaviour of masonry-infilled RC frames strengthened using textile reinforced mortar: an experimental and numerical studies overview", *Journal of Earthquake Engineering*, 26(15), pp. 7743–7767, 2022.
<https://doi.org/10.1080/13632469.2021.1988763>

7 Conflict of interest

The authors have no conflict to declare.